Electronic Supplementary Material (ESI) for Environmental Science: Processes & Impacts.

Supporting Information for:

Precipitation of aqueous transition metals in particulate matter during the dithiothreitol (DTT) oxidative potential assay

Jayashree Yalamanchili, Christopher J. Hennigan, Brian E. Reed**

Department of Chemical, Biochemical and Environmental Engineering, University of Maryland, Baltimore County, 1000 Hilltop Circle, Baltimore, Maryland 21250, United States.

To whom correspondence should be addressed: C.J. Hennigan. Email: hennigan@umbc.edu; phone: (410) 455-3515. B.E. Reed. Email: reedb@umbc.edu; phone: (410) 455-8154.

Contents of this file:

Pages: 43

Figures S1/S7

Tables S1/S9

List of figures:

List of tables:

(a)

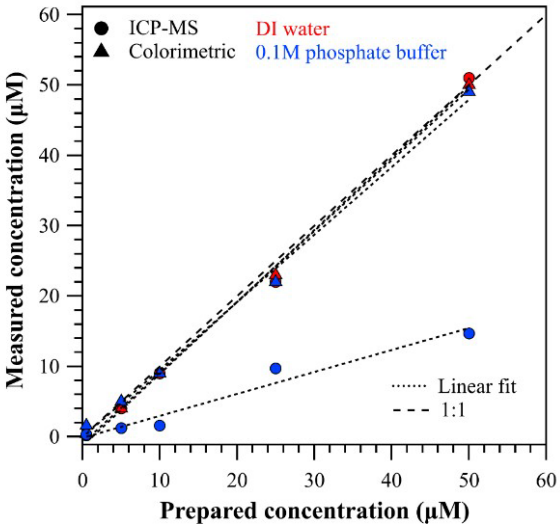
ICP-MS
Colorimetric
DI water
0.1M phosphate buffer
Linear fit
1:1
Measured concentration (μM)
Prepared concentration (μM)
0
10
20
30
40
50
60

(b)

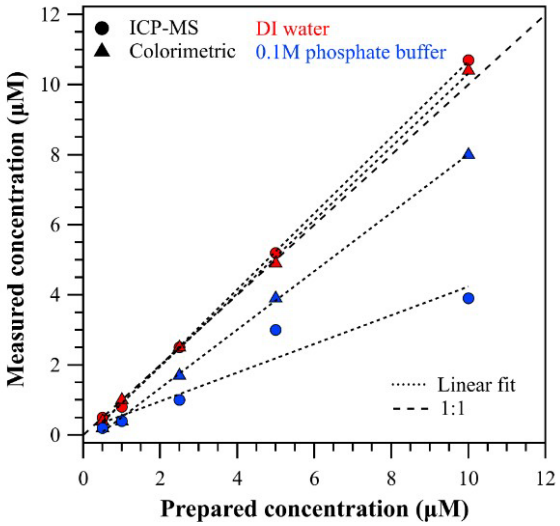
ICP-MS
Colorimetric
DI water
0.1M phosphate buffer
Linear fit
1:1
Measured concentration (μM)
Prepared concentration (μM)
0
2
4
6
8
10
12

(c)

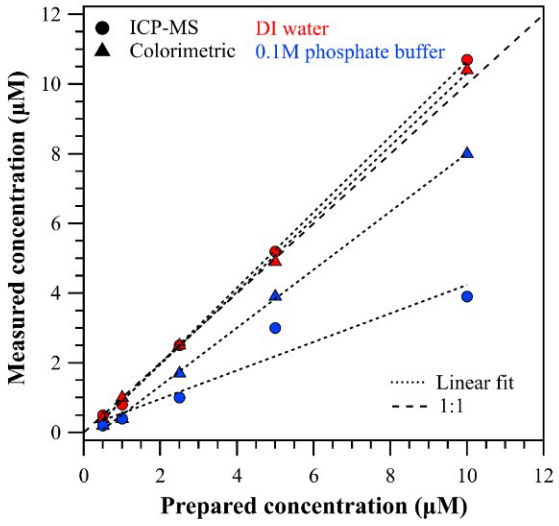
ICP-MS
Colorimetric
DI water
0.1M phosphate buffer
Linear fit
1:1
Measured concentration (μM)
Prepared concentration (μM)
0
2
4
6
8
10
12

Figure S1. Calibration curves for (a) Fe (b) Mn and (c) Cu comparing the prepared concentration to the measured concentrations using both ICP-MS and colorimetric analysis. Calibration curves for each of the metals were measured in DI water (red data points) and 0.1 M phosphate buffer (blue data points). Colorimetric Fe analysis was not affected by the presence of phosphate; however, the response of Mn and Cu decreased slightly in 0.1M phosphate buffer matrix compared to their measurement in DI water. Calibration curves for Mn and Cu in 0.1M phosphate buffer matrix were used for their colorimetric measurements in the DTT assay. The figures of merit for the calibration curves are given in Table S3-S5. The method detection limits for the colorimetric analyses are in Table S6.

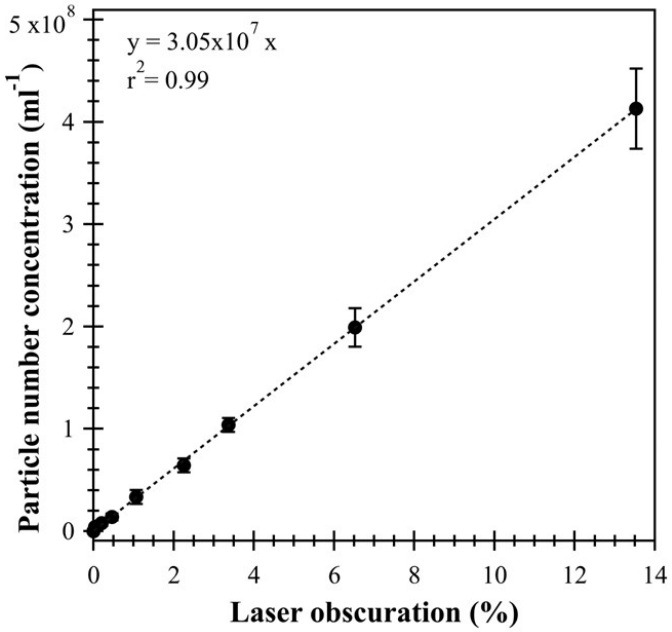

Figure S2. Particle number concentration of PSL in DI water as a function of the laser obscuration measured using the laser particle light scattering analysis. The particle light scattering measurements were limited to quantifying the particle number concentration because particle mass concentration measurements require knowledge of the precipitate identity and optical properties (i.e., refractive index). The detection limit was 3.97 x 10^6 ml^{-1}.

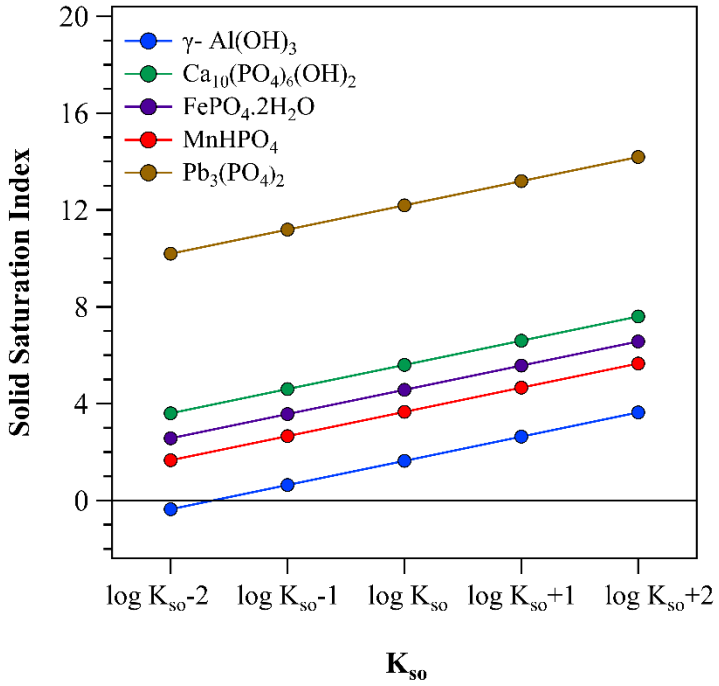

Figure S3. Effect of K_{s0} on saturation index for Al, Ca, Fe(III), Mn and Pb precipitation for SRM-1648a sample 3 at the assay conditions (0.1 M phosphate buffer, pH 7.4, 37 °C). Note that saturation index (SI) = log(ion activity product/solubility product). A positive value of SI indicates that precipitation is thermodynamically possible.

(a)

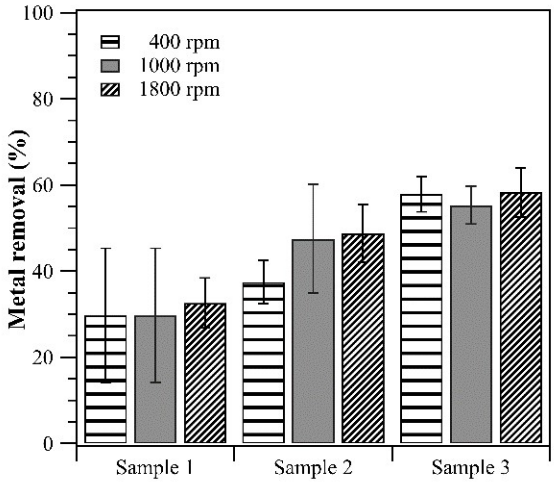

(b)

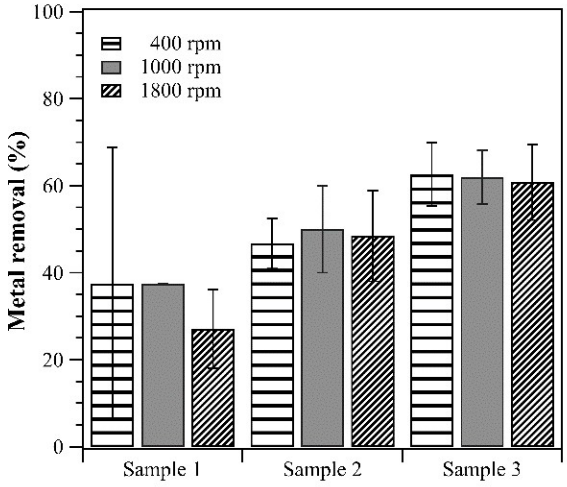

Figure S4. Effect of the mixing speed on Fe removal in SRM-1648a extract samples 1, 2, and 3 during the (a) presence and (b) absence of DTT under the assay conditions (0.1 M phosphate buffer, pH 7.4, 37 ±3 °C) for 30 minutes. The mixing speed did not have any effect on the extent of Fe removal.

(a)

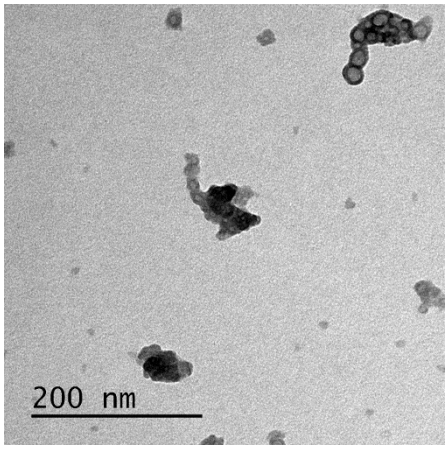

(d)

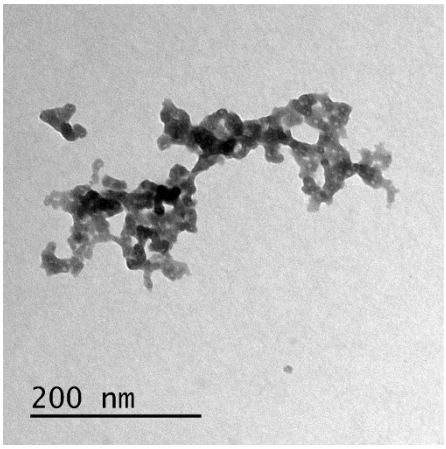

(b)

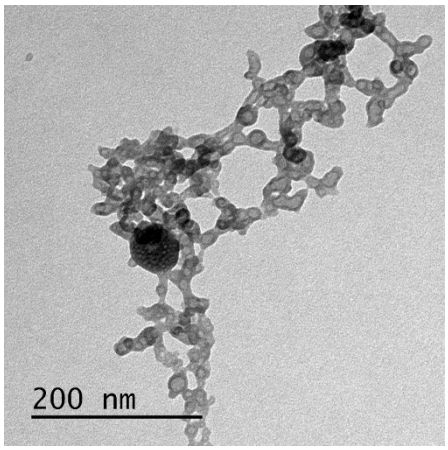

(e)

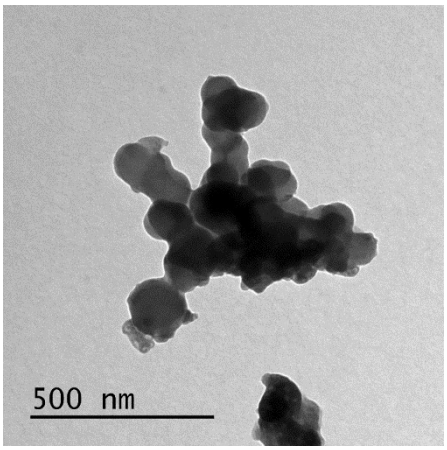

(c)

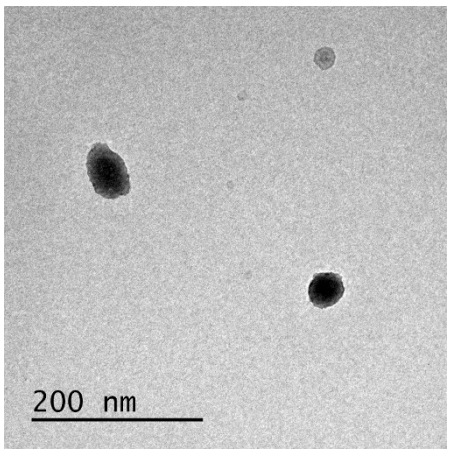

(f)

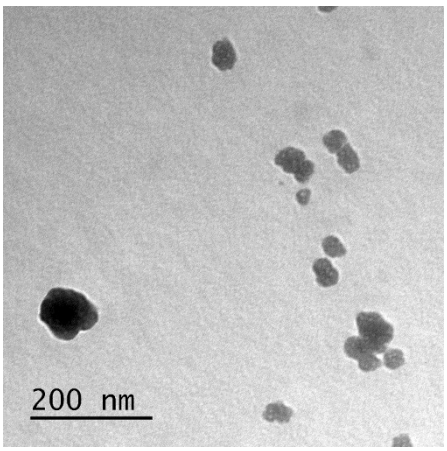

Figure S5. Solids of size ~200- 500nm are identified by the TEM images of the SRM1648a extract samples filtered after 30 minutes in the DTT assay (0.1M phosphate buffer, pH 7.4, 37 ±3 °C) for (a) sample 1 (b) sample 2 and (c) sample 3 in the presence of DTT,
(d) sample 1, (e) sample 2 and (f) sample 3 in the absence of DTT.

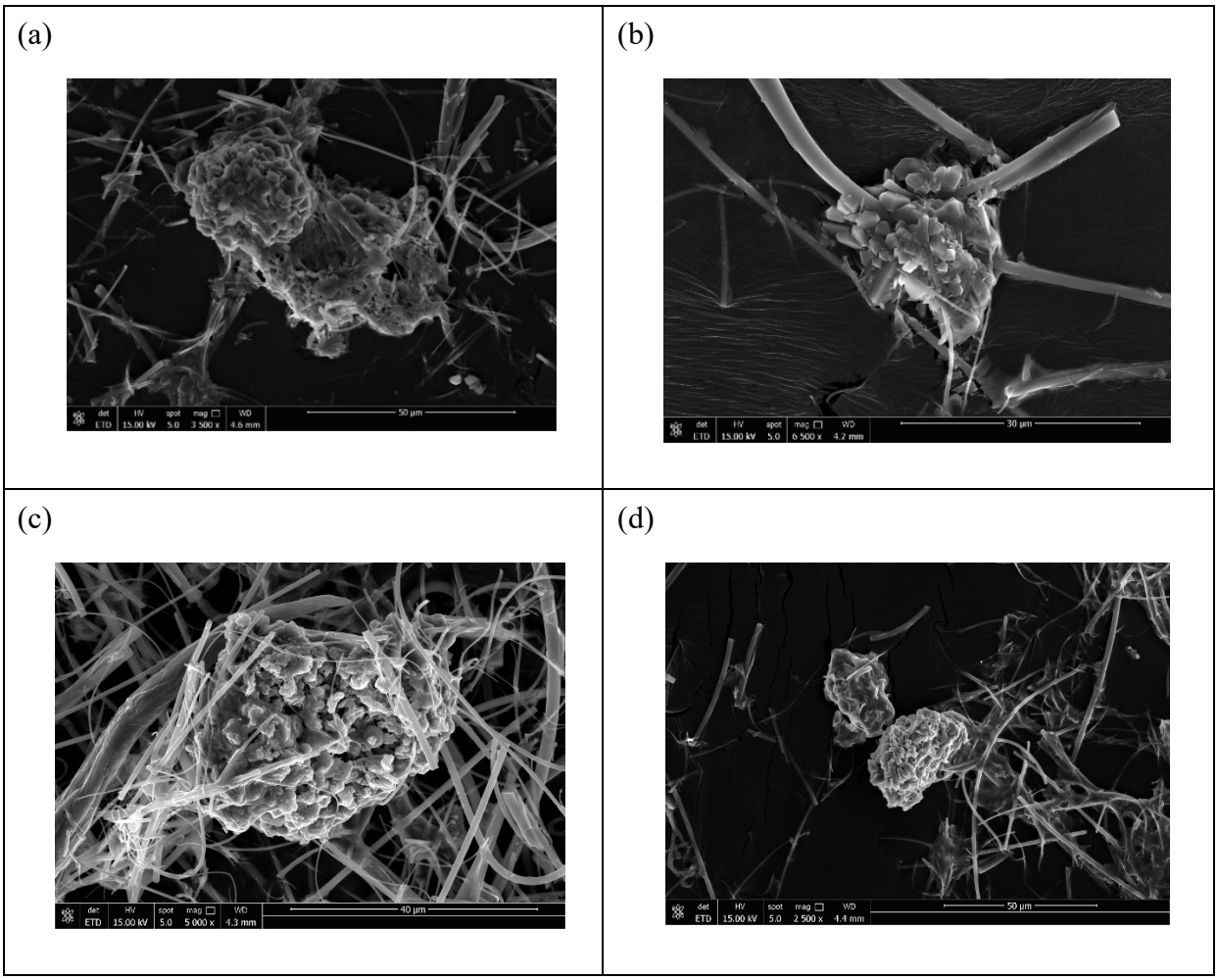

Figure S6. SEM images of the SRM-1648a extract samples filtered after 30 minutes in the DTT assay (0.1M phosphate buffer, pH 7.4, 37 ±3 °C) for (a) sample 2 in the absence of DTT, (b) sample 2 in the presence of DTT, (c) sample 3 in the absence of DTT (d) sample 3 in the presence of DTT shows solid clusters that were used for EDS analysis.

(a)

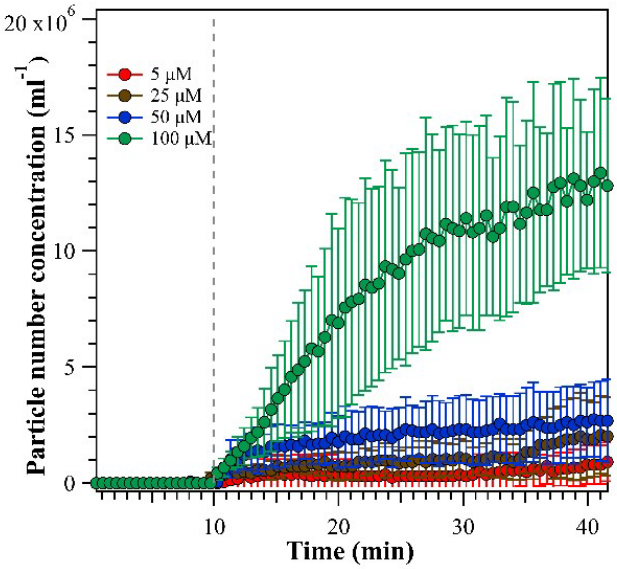
20 x10^6
Particle number concentration (ml^-1)
5 µM
25 µM
50 µM
100 µM
0
5
10
15
10
20
30
40
Time (min)

(b)

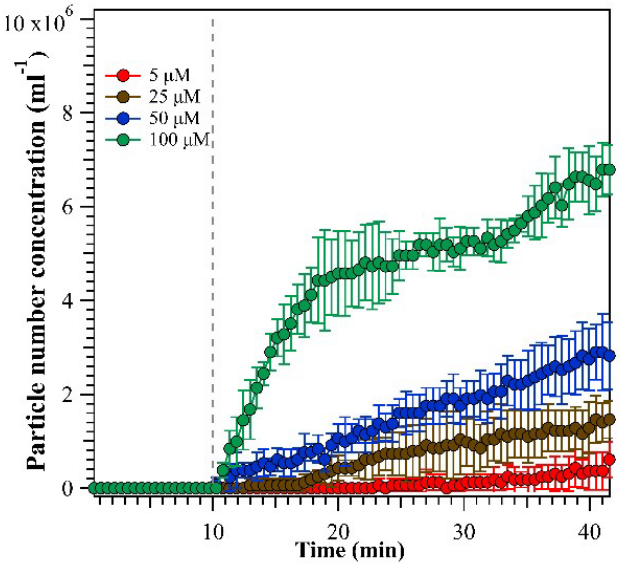
10 x10^6
Particle number concentration (ml^-1)
5 µM
25 µM
50 µM
100 µM
0
2
4
6
8
10
20
30
40
Time (min)

(c)

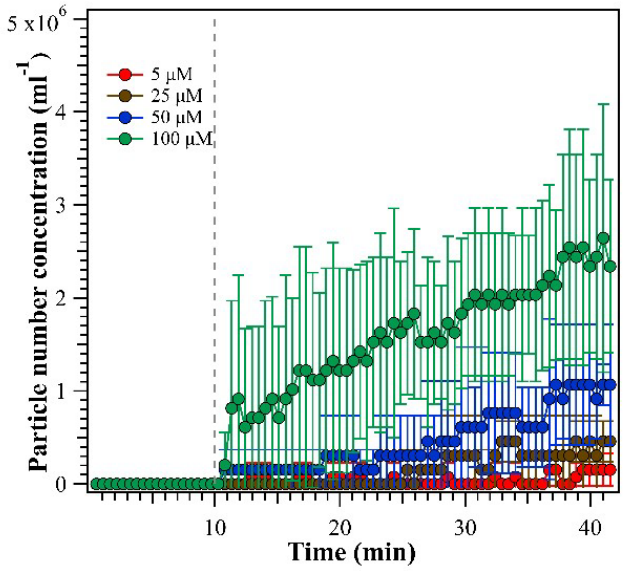

Figure S7. Particle number concentration for each of the individual metal-salt experiments of (a) Fe(III), (b) Fe(II) and (c) Mn(II) in the DTT assay (0.1M phosphate buffer, pH 7.4 and 37± 3 °C) measured in Figure 4(a) as a function of the initial metal concentration. Symbols represent the mean values and error bars represent the standard deviation of measurements performed in triplicate.

Table S1. Certified Mass Fraction Values (Dry-Mass Basis) of all elements present in NIST Urban Particulate matter SRM-1648a as given in the NIST database.

Element	Mass fraction (% or mg/kg)
Aluminum (Al)(a,b)	3.43 ± 0.13 %
Antimony (Sb)(a,c)	45.4 ± 1.4 mg/kg
Arsenic (As)(a,c,d,e)	115.5 ± 3.9 mg/kg
Bromine (Br)(a,b,e)	502 ± 10 mg/kg
Calcium (Ca)(a,b,c,e)	5.84 ± 0.19 %
Cadmium (Cd)(d,f)	73.7 ± 2.3 mg/kg
Cerium (Ce)(a,c)	54.6 ± 2.2 mg/kg
Chlorine (Cl)(a,b)	4543 ± 47 mg/kg
Cobalt (Co)(a,c)	17.93 ± 0.68 mg/kg
Chromium (Cr)(a,b)	402 ± 13 mg/kg
Copper (Cu)(a,d,e)	610 ± 70 mg/kg
Iron (Fe)(a,b,e,f)	3.92 ± 0.21 %
Lead (Pb)(b,c,d,e)	0.655 ± 0.033 %
Magnesium (Mg)(a,b)	0.813 ± 0.012 %
Manganese (Mn)(a,b,e)	790 ± 44 mg/kg
Mercury (Hg)(g)	1.323 ± 0.064 mg/kg
Nickel (Ni)(b,c,d,e)	81.1 ± 6.8 mg/kg

Potassium (K)(a,b,e,f)	1.056 ± 0.049 %
Rubidium (Rb)(a,c)	51.0 ± 1.5 mg/kg
Sodium (Na)(a,b)	4240 ± 60 mg/kg
Strontium (Sr)(b,e)	215 ± 17 mg/kg
Sulfur (S)(b,f)	5.51 ± 0.36 %
Titanium (Ti)(a,b,c,e,f)	4021 ± 86 mg/kg
Vanadium (V)(a,e)	127 ± 11 mg/kg
Zinc (Zn)(a,b,c,d,e)	4800 ± 270 mg/kg
(a) INAA (NIST) (b) WDXRF (NIST) (c) PAA (d) SSGFAAS (e) PIXE (f) PGAA (NIST) (g) Isotope dilution ICP-MS (NIST)	

Table S2. Comparison of colorimetric and ICP-MS measurements for Fe, Cu, and Mn for an SRM-1648a extract.

Metal	Extract concentration, μM		Extraction Efficiency (%)	
Method	Colorimetric	ICP-MS	Colorimetric	ICP-MS
TOTFe	125.4	105.9	17.9	15.1
Cu	4.2	4.5	44.3	46.9
Mn	6.6	6.7	45.6	46.5

Table S3. Slope, intercept, and R-square for colorimetric method calibration for Fe in the DI water and 0.1M phosphate buffer matrix.

Method	ICP-MS analysis		Colorimetric analysis	
Fe, μM	DI water	0.1M phosphate buffer	DI water	0.1M phosphate buffer
R^2	0.994	0.959	0.997	0.995
Slope	1.03	0.31	1.01	0.97
Intercept	-1.34	-0.17	-0.89	-0.15

Table S4. Slope, intercept, and R-square for colorimetric method calibration for Mn in the DI water and 0.1M phosphate buffer matrix.

Method	ICP-MS analysis		Colorimetric analysis	
Mn, μM	DI water	0.1M phosphate buffer	DI water	0.1M phosphate buffer
R^2	0.9997	0.917	0.999	0.999
Slope	1.09	0.41	1.05	0.84
Intercept	-0.18	0.17	-0.12	-0.33

Table S5. Slope, intercept, and R-square for colorimetric method calibration for Cu in the DI water and 0.1M phosphate buffer matrix.

Method	ICP-MS analysis		Colorimetric analysis	
Cu, µM	DI water	0.1M phosphate buffer	DI water	0.1M phosphate buffer
R^2	0.9999	0.871	0.999	0.997
Slope	0.98	0.39	0.96	0.78
Intercept	-0.13	0.22	0.03	-0.60

Table S6. Method Detection limit for the colorimetric analysis in DI water and 0.1M phosphate buffer matrices.

Method/ matrix	Total Fe, µM	Fe(II), µM	Mn(II), µM	Cu(II), µM
DI water	0.5	0.5	0.5	0.5
0.1M phosphate buffer	0.5	0.5	1.0	1.4

Table S7. Thermodynamic data for the metals in their aqueous phase complexes and solid forms at 25°C. The thermodynamic data in MINEQL was supplemented from the NIST database to account for all possible complexes and solids. Note that all modeling was done at 37 °C as MINEQL corrects the equilibrium constants for temperature and ionic strength using the Van't Hoff and Davies equation respectively.

Cu(I)	**H_2O**	**H^+**	**CO_3^{2-}**	**Cu^{1+}**	**PO_4^{3-}**	**log k**	**delta H**
Solids							
Cuprite	1	-2	0	2	0	1.406	29.642
Cu(II)	**H_2O**	**H^+**	**CO_3^{2-}**	**Cu^{2+}**	**PO_4^{3-}**	**log k**	**delta H**
Aqueous							
$Cu(OH)_2$	2	-2	0	1	0	-16.194	0
$Cu_2(OH)_2^{+2}$	2	-2	0	2	0	-10.594	18.313
$Cu(OH)_4^{-2}$	4	-4	0	1	0	-39.98	0
$Cu(OH)^+$	1	-1	0	1	0	-7.497	8.559
$Cu(OH)_3^-$	3	-3	0	1	0	-26.879	0
$CuHCO_3^+$	0	1	1	1	0	12.129	0
$CuCO_3$	0	0	1	1	0	6.77	0

$Cu(CO_3)_2^{-2}$	0	0	2	1	0	10.2	0
$CuHPO_4$	0	1	0	1	1	16.5	0
Solids							
Azurite	2	-2	2	3	0	16.906	22.758
Malachite	2	-2	1	2	0	5.306	-18.255
Tenorite	1	-2	0	1	0	-7.644	15.504
$Cu(OH)_2$	2	-2	0	1	0	-8.674	13.485
$Cu_3(PO_4)_2{:}3H_2O$	3	0	0	3	2	35.12	0
$CuCO_3$	0	0	1	1	1	11.5	0
$Cu_3(PO_4)_2$	0	0	0	3	2	36.85	0
Fe(III)	**H_2O**	**H^+**	**CO_3^{2-}**	**Fe^{3+}**	**PO_4^{3-}**	**log k**	**delta H**
Aqueous							
$Fe_3(OH)_4^{+5}$	4	-4	0	3	0	-6.288	15.593
$Fe(OH)_4^-$	4	-4	0	1	0	-21.588	0
$Fe(OH)_3$	3	-3	0	1	0	-12.56	24.809
$Fe_2(OH)_2^{+4}$	2	-2	0	2	0	-2.854	13.771

$Fe(OH)_2^+$	2	2	0	1	0	-4.954	0
$FeOH^{+2}$	1	-1	0	1	0	-2.187	9.993
$FeHPO_4^+$	0	1	0	1	1	22.292	-7.3
$FeH_2PO_4^{+2}$	0	2	0	1	1	23.852	0
Solids							
Goethite	2	-3	0	1	0	-0.491	14.48
Lepidocrocite	2	-3	0	1	0	-1.371	0
Hematite	3	-6	0	2	0	1.418	30.829
Ferrihydrite	3	-3	0	1	0	-3.191	17.573
Maghemite	3	-6	0	2	0	-6.386	0
Strengite	2	0	0	1	1	26.4	2.237
Fe(II)	**H_2O**	**H^+**	**CO_3^{2-}**	**Fe^{2+}**	**PO_4^{3-}**	**log k**	**delta H**
Aqueous							
$FeOH^+$	1	-1	0	1	0	-9.397	13.339
$Fe(OH)_2$	2	-2	0	1	0	-20.494	28.59
$Fe(OH)_3^-$	3	-3	0	1	0	-28.991	30.218

$FeHCO_3^+$	0	1	1	1	0	11.429	0
$FeH_2PO_4^+$	0	2	0	1	1	22.273	0
$FeHPO_4$	0	1	0	1	1	15.975	0
Solids							
Wusite	1	-2	0	0.95	0	-11.688	24.842
$Fe(OH)_2$	2	-2	0	1	0	-13.564	0
Vivianite	8	0	0	3	2	36	0
Siderite	0	0	1	1	0	10.24	3.824
$Fe_3(PO_4)_2$	0	0	0	3	2	36	0
Mn(II)	**H_2O**	**H^+**	**CO_3^{2-}**	**Mn^{2+}**	**PO_4^{3-}**	**log k**	**delta H**
Aqueous							
$Mn(OH)_4^{-2}$	4	-4	0	1	0	-48.28	0
$MnOH^+$	1	-1	0	1	0	-10.597	13.339
$Mn(OH)_3^-$	3	-3	0	1	0	-34.8	0
$MnHCO_3^+$	0	1	1	1	0	11.629	-2.534
$MnCO_3$	0	0	1	1	0	4.7	0

$MnHPO_4$	0	1	0	1	1	15.8	0
Solids							
Pyrochroite	2	-2	0	1	0	-15.194	23.186
$MnHPO_4$	0	1	0	1	1	25.4	0
Rhodochrosite	0	0	1	1	0	10.58	0.449
$Mn_3(PO_4)_2$	0	0	0	3	2	23.827	-2.12
Mn(III)	**H_2O**	**H^+**	**CO_3^{2-}**	**Mn^{3+}**	**PO_4^{3-}**	**log k**	**delta H**
Solids							
Bixbyite	3	-6	0	2	0	0.644	29.754
Mn(IV)	**H_2O**	**H^+**	**CO_3^{2-}**	**Mn^{2+}**	**PO_4^{3-}**	**log k**	**delta H**
Solids							
Manganite	2	-3	0	1	0	-25.34	0
Ni(II)	**H_2O**	**H^+**	**CO_3^{2-}**	**Ni^{2+}**	**PO_4^{3-}**	**log k**	**delta H**
Aqueous							
$Ni(OH)_2$ (aq)	2	-2	0	1	0	-18.994	0
$Ni(OH)_3^-$	3	-3	0	1	0	-29.991	0

$NiCO_3$ (aq)	0	0	1	1	0	4.572	0
$NiH_2PO_4^+$	0	2	0	1	1	20.5	0
$NiHCO_3^+$	0	1	1	1	0	12.42	0
$NiHPO_4$ (aq)	0	1	0	1	1	15.33	0
$NiOH^+$	1	-1	0	1	0	-9.897	12.383
Solids							
Bunsenite	1	-2	0	1	0	-12.446	23.932
$Ni(OH)_2$	2	-2	0	1	0	-12.794	22.935
$NiCO_3$	0	0	1	1	0	6.87	9.94
$Ni_3(PO_4)_2$	0	0	0	3	2	31.3	0
Zn(II)	**H_2O**	**H^+**	**CO_3^{2-}**	**Zn^{2+}**	**PO_4^{3-}**	**log k**	**delta H**
Aqueous							
$Zn(CO_3)_2^{-2}$	0	0	2	1	0	7.3	0
$Zn(OH)_2$ (aq)	2	-2	0	1	0	-17.794	0
$Zn(OH)_3^-$	3	-3	0	1	0	-28.091	0
$Zn(OH)_4^{-2}$	4	-4	0	1	0	-40.488	0

$Zn(CO_3)_2$	0	1	0	1	1	7.3	0
$ZnCO_3$ (aq)	0	0	1	1	0	4.76	0
$ZnHCO_3^+$	0	1	1	1	0	11.829	0
$ZnHPO_4$ (aq)	0	1	0	1	1	15.69	0
$ZnOH^+$	1	-1	0	1	0	-8.997	13.339
Solids							
$Zn(OH)_2$ [Am]	2	-2	0	1	0	-12.474	19.269
Zincite	1	-2	0	1	0	-11.334	21.42
$Zn(OH)_2$	2	-2	0	1	0	-12.2	0
ZnO (active)	1	-2	0	1	0	-11.188	21.214
$ZnCO_3$:1H_2O	1	0	1	1	0	10.26	0
$Zn_3(PO_4)_2$:4H_2O	4	0	0	3	2	35.42	0
Smithsonite	0	0	1	1	0	10	3.786
$Zn_3(PO_4)_2$	0	0	0	3	2	35.42	0
Cr(III)	**H_2O**	**H^+**	**CO_3^{2-}**	**$Cr(OH)^{2+}$**	**PO_4^{3-}**	**log k**	**delta H**

Aqueous							
$Cr(OH)_3$ (aq)	1	-1	0	1	0	-8.422	0
$Cr(OH)_4^-$	2	-2	0	1	0	-17.819	0
$CrH_2PO_4^{+2}$	-2	4	0	1	1	31.907	0
$CrOH^{+2}$	-1	1	0	1	0	5.912	-18.621
Solids							
$Cr(OH)_3$ [Am]	1	-1	0	1	0	0.75	0
$Cr(OH)_3$	1	-1	0	1	0	-1.336	7.115
Cr_2O_3	-1	-2	0	2	0	2.358	12.125
Cr(VI)	**H_2O**	**H^+**	**CO_3^{2-}**	**$CrO_4^{(2-}$)**	**PO_4^{3-}**	**log k**	**delta H**
Aqueous							
$CrO_3H_2PO_4^-$	-1	4	0	1	1	29.363	0
$CrO_3HPO_4^{-2}$	-1	3	0	1	1	26.681	0
$Cr_2O_7^{-2}$	-1	2	0	2	0	14.56	-3.585
Solids							

CrO_3	-1	2	0	1	0	3.21	1.245
Co(II)	**H_2O**	**H^+**	**CO_3^{2-}**	**Co^{2+}**	**PO_4^{3-}**	**log k**	**delta H**
Aqueous							
$Co(OH)_2$ (aq)	2	-2	0	1	0	-18.794	0
$Co(OH)_3^-$	3	-3	0	1	0	-31.491	0
$Co4(OH)_4^{+4}$	4	-4	0	4	0	-30.488	0
$CoCO_3$ (aq)	0	0	1	1	0	4.228	0
$CoHCO_3^+$	0	1	1	1	0	12.22	0
$CoHPO_4$ (aq)	0	1	0	1	1	15.413	0
$CoOH^+$	1	-1	0	1	0	-9.697	0
Solids							
CoO	1	-2	0	1	0	-13.586	25.405
$Co(OH)_2$	2	-2	0	1	0	-13.094	0
$CoHPO_4$	0	1	0	1	1	19.061	0
$CoCO_3$	0	0	1	1	0	9.98	3.05
$Co_3(PO_4)_2$	0	0	0	3	2	34.688	0

Co(III)	**H_2O**	**H^+**	**CO_3^{2-}**	**Co^{3+}**	**PO_4^{3-}**	**log k**	**delta H**
Aqueous							
$CoOH^{+2}$	1	-1	0	1	0	-1.291	0
Solids							
$Co(OH)_3$	3	-3	0	1	0	2.309	22.091
V(III)	**H_2O**	**H^+**	**CO_3^{2-}**	**V^{3+}**	**PO_4^{3-}**	**log k**	**delta H**
Aqueous							
$V(OH)_3$ (aq)	3	-3	0	1	0	-3.084	0
$V2(OH)_3^{+3}$	3	-3	0	2	0	-10.119	0
$V(OH)_2^{+}$	2	-2	0	1	0	-6.274	0
VOH^{+2}	1	-1	0	1	0	-2.297	10.471
$V_2(OH)_2^{+4}$	2	-2	0	2	0	3.794	0
Solids							
V_2O_3	1.5	-3	0	0	1	-4.9	19.72
$V(OH)_3$	3	-3	0	0	1	-7.591	0
Al(III)	**H_2O**	**H^+**	**CO_3^{2-}**	**Al^{3+}**	**PO_4^{3-}**	**log k**	**delta H**

Aqueous							
$Al(OH)_2$	2	-2	0	1	0	-10.094	0
$Al(OH)_3$ (aq)	3	-3	0	1	0	-16.791	0
$Al(OH)_4$	4	-4	0	1	0	-22.688	41.405
AlOH	1	-1	0	1	0	-4.997	11.427
$Al_2(OH)_2CO_3$	2	-2	1	2	0	-4.31	0
Al_2PO_4	0	0	0	2	1	-18.98	0
Solids							
Diaspore	2	-3	0	1	0	-6.873	24.63
Al_2O_3	3	-6	0	2	0	-19.652	61.805
Boehmite	2	-3	0	1	0	-8.578	28.13
$Al(OH)_3$ [am]	3	-3	0	1	0	-10.8	26.53
Gibbsite	3	-3	0	1	0	-8.291	22.8
Ca(II)	**H_2O**	**H^+**	**CO_3^{2-}**	**Ca^{2+}**	**PO_4^{3-}**	**log k**	**delta H**
Aqueous							
CaOH	1	-1	0	1	0	-12.697	15.323

$CaHCO_3^+$	0	1	1	1	0	11.599	1.291
$CaH_2PO_4^+$	0	2	0	1	1	20.923	-1.434
$CaHPO_4$ (aq)	0	1	0	1	1	15.035	-0.717
$CaCO_3$ (aq)	0	0	1	1	0	3.2	3.824
$CaPO_4^-$	0	0	0	1	1	6.46	3.1
Solids							
Lime	1	-2	0	1	0	-32.699	46.346
Portlandite	2	-2	0	1	0	-22.804	30.741
Hydroxylapatite	1	-1	0	5	3	44.333	0
$CaHPO_4{:}2H_2O$	2	1	0	1	1	18.995	-5.497
$Ca_4H(PO_4)_3{:}3H_2O$	3	1	0	4	3	47.08	0
$CaHPO_4$	0	1	0	1	1	19.275	-7.409
Aragonite	0	0	1	1	0	8.3	2.868
Calcite	0	0	1	1	0	8.48	1.912
$Ca_3(PO_4)_2$ (β)	0	0	0	3	2	28.92	-12.906
Mg(II)	**H_2O**	**H^+**	**CO_3^{2-}**	**Mg^{2+}**	**PO_4^{3-}**	**log k**	**delta H**

Aqueous							
$MgOH^+$	1	-1	0	1	0	-11.397	16.207
$MgHCO_3^+$	0	1	1	1	0	11.339	-2.534
$MgHPO_4$ (aq)	0	2	0	1	1	15.175	-0.717
$MgH_2PO_4^+$	0	2	0	1	1	21.256	-1.12
$MgCO_3$ (aq)	0	0	1	1	0	2.92	2.868
$MgPO_4^-$	0	0	0	1	1	4.654	3.1
Solids							
Hydromagnesite	6	-2	4	5	0	8.766	52.21
Artinite	5	-2	1	2	0	-9.6	28.742
$Mg(OH)_2$ (active)	2	-2	0	1	0	-18.794	0
Periclase	1	-2	0	1	0	-21.584	36.145
Brucite	2	-2	0	1	0	-16.844	27.246
$MgHPO_4{:}3H_2O$	3	1	0	1	1	18.175	0
Nesquehonite	3	0	1	1	0	4.67	5.789
Magnesite	0	0	1	1	0	7.46	-4.78

$Mg_3(PO_4)_2$	0	0	0	3	2	23.28	0
Mo(II)	**H_2O**	**H^+**	**CO_3^{2-}**	**MoO_4^{2-}**	**PO_4^{3-}**	**log k**	**delta H**
Aqueous							
$H_2Mo_7O_{24}^{-4}$	-4	10	0	7	0	64.159	-51.386
$Mo_7O_{24}^{-6}$	-4	8	0	7	0	52.99	-54.493
$HMo_7O_{24}^{-5}$	-4	9	0	7	0	59.377	-52.103
$H_3Mo_7O_{24}^{-3}$	-4	11	0	7	0	67.405	-51.864
$HMoO_4^-$	0	1	0	1	0	4.299	4.78
H_2MoO_4 (aq)	0	2	0	1	0	8.164	-6.214
Solids							
MoO_3	-1	2	0	1	0	8	0
H_2MoO_4	0	2	0	1	0	12.876	-11.711
Pb(II)	**H_2O**	**H^+**	**CO_3^{2-}**	**Pb^{2+}**	**PO_4^{3-}**	**log k**	**delta H**
Aqueous							
$Pb(OH)_2$ (aq)	2	-2	0	1	0	-17.094	0
Pb_2OH^{+3}	1	-2	0	2	0	-6.397	0

$Pb(OH)_3^-$	3	-3	0	1	0	-28.091	0
$PbOH^+$	1	-1	0	1	0	-7.597	0
$Pb(OH)_4^{-2}$	4	-4	0	1	0	-39.699	0
$Pb_3(OH)_4^{+2}$	4	-4	0	3	0	-23.888	27.543
$Pb_4(OH)_4^{+4}$	4	-4	0	4	0	-19.988	21.09
$PbHCO_3^+$	0	1	1	1	0	13.2	0
$PbCO_3$ (aq)	0	0	1	0	0	6.478	0
$Pb(CO_3)_2^{-2}$	0	0	2	1	0	9.938	0
$PbPO_4H_2$	0	2	0	1	1	-21.073	0
$PbPO_4H$	0	1	0	1	1	-15.475	0
Solids							
$Pb_{10}(OH)_6O(CO_3)_6$	7	-8	6	10	0	6.76	0
$Pb_3O_2CO_3$	2	-4	1	3	0	-11.02	26.43
Pb_2OCO_3	1	-2	1	2	0	0.558	9.756
Hydrocerrusite	2	-2	2	3	0	18.77	0
Litharge	1	-2	0	1	0	-12.694	15.655

$Pb(OH)_2$	2	-2	0	1	0	-8.15	13.99
Massicot	1	-2	0	1	0	-12.894	15.977
$Pb_2O(OH)_2$	3	-4	0	2	0	-26.188	0
$PbO:0.3H_2O$	1.33	-2	0	1	0	-12.98	0
Hydroxylpyromorphite	1	-2	0	5	3	62.79	0
$PbHPO_4$	0	1	0	1	1	23.805	0
Cerrusite	0	0	1	1	0	13.13	-5.925
$Pb_3(PO_4)_2$	0	0	0	3	2	43.53	0

Table S8. Solubilities of various precipitates for each metal under assay conditions (0.1M PO_4, ionic strength=0.22, 37C, fixed solids). Three types of solids were considered: metal oxides, hydroxides, and phosphate-based solids based on previous work [36].

Metal	Solid	Solubility(μM)	pC, M
Cu(I)	Cuprite (Cu_2O)	$4.1x\ 10^{-3}$	-8.4
Cu(II)	$Cu_3(PO_4)_2$	4.5	-5.3
	Tenorite (CuO)	9.8	-5.0
	$Cu_3(PO_4)_2{:}3H_2O$	$1.7x10^{1}$	-4.8
	$Cu(OH)_2$	$1.2x10^{2}$	-3.9
Fe(II)	$Fe_3(PO_4)_2$	2.9	-5.5
	Vivianite ($Fe_3(PO_4)_2{:}8H_2O$)	2.9	-5.5
	Wusite (FeO)	$1.1x10^{4}$	-2.0
	$Fe(OH)_2$	$3.1x10^{5}$	-0.5
Fe(III)	Hematite (Fe_2O_3)	$2.0x10^{-7}$	-12.7
	Goethite (ὰ- FeO(OH))	$3.4x10^{-6}$	-11.5
	Lepidocrocite ($_\gamma$ - FeO(OH))	$6.6x10^{-5}$	-10.2
	Strengite ($FePO_4.2H_2O$)	$5.1x10^{-4}$	-9.3
	Ferrihydrite ($Fe_2O_3.0.5H_2O$)	$1.4x10^{-3}$	-8.9

	Maghemite ($_{\gamma}$ - Fe_2O_3)	$4.4x10^{-3}$	-8.4
Mn(II)	$MnHPO_4$	$2.6x10^{-4}$	-9.6
	$Mn_3(PO_4)_2$	$2.1x10^{4}$	-1.7
	Pyrochroite ($Mn(OH)_2$)	$2.1x10^{6}$	0.3
	Hausmannite ($(Mn^{2+}\ Mn^{3+})_2\ O_4$)	$2.5x10^{-1}$	-6.6
Mn(III)	Manganite ($MnO(OH)$)	$6.4x10^{-2}$	-7.2
	Bixbyite ($(Mn, Fe)_2O_3$)	$2.0x10^{-16}$	-21.7
Mn(IV)	Pyrolusite (MnO_2)	$2.3x10^{-7}$	-12.6
	Nsutite ($Mn^{4+}\ Mn^{2+}O(OH)_2$)	$8.4x10^{-18}$	-23.1
	Birnessite ($(Mn^{4+}\ Mn^{3+})_2O_2.5H_2O$)	$3.2x10^{-17}$	-22.5
Ni(II)	$Ni_3(PO_4)_2$	$2.4x10^{1}$	-4.6
	Bunsenite (NiO)	$2.3x10^{4}$	-1.6
	$Ni(OH)_2$	$4.4x10^{4}$	-1.4
Zn(II)	$Zn_3(PO_4)_2$	2.2	-5.7
	$Zn(OH)_2$	$6.9x10^{4}$	-1.2
Cr(III)	Cr_2O_3	$2.7x10^{-3}$	-8.6
	$Cr(OH)_3$ [Am]	$1.1x10^{-2}$	-8.0
	$Cr(OH)_3$	$8.2x10^{-1}$	-6.1

Cr(VI)	CrO_3	$4.2x10^{29}$	23.6
Co(II)	$Co_3(PO_4)_2$	2.1	-5.7
	$CoHPO_4$	$2.5x10^{2}$	-3.6
	CoO	$1.2x10^{5}$	-0.9
	$Co(OH)_2$	$1.6x10^{5}$	-0.8
Co(III)	$Co(OH)_3$	$3.4x10^{-13}$	-18.5
V(III)	V_2O_3	$1.8x10^{7}$	1.3
	$V(OH)_3$	$3.2x10^{10}$	4.5
Al(III)	Diaspore (AlO(OH))	$1.6x10^{-2}$	-7.8
	Gibbsite (γ- $Al(OH)_3$)	$4.7x10^{-1}$	-6.3
	Boehmite (AlO(OH))	$6.4x10^{-1}$	-6.2
	Al_2O_3	9.5	-5.0
	$Al(OH)_3$ [Am]	$1.2x10^{2}$	-3.9
Ca(II)	Hydroxylpatite ($Ca_{10}(PO_4)_6(OH)_2$)	6.6	-5.2
	$Ca_3(PO_4)_2$	$1.2x10^{2}$	-3.9
	$CaHPO_4$	$1.3x10^{2}$	-3.9
	$Ca_4H(PO_4)_3{:}3H_2O$	$1.7x10^{2}$	-3.8
	$CaHPO_4{:}2H_2O$	$2.2x10^{2}$	-3.7

	Calcite (metastable $Ca(CO_3)$)	$7.1x10^3$	-2.1
	Aragonite ($CaCO_3$)	$8.5x10^3$	-2.1
	Portlandite (metastable $Ca(OH)_2$)	$4.9x10^{13}$	7.7
	Lime ($Ca(OH)_2$)	$1.4x10^{23}$	17.1
Mg(II)	$MgHPO_4:3H_2O$	$1.2x10^3$	-2.9
	$Mg_3(PO_4)_2$	$8.4x10^3$	-2.1
	Magnesite ($MgCO_3$)	$2.9x10^4$	-1.5
	Hydromagnesite ($Mg_5(CO_3)_4(OH)_2.4H_2$)	$1.5x10^5$	-0.8
	Nesquehonite ($MgHCO_3(OH).2H_2O$)	$4.4x10^5$	-0.4
	Artinite ($Mg_2(OH)_2.3H_2O$)	$5.3x10^5$	-0.3
	Brucite ($Mg(OH)_2$)	$6.8x10^7$	1.8
	$Mg(OH)_2$	$3.6x10^{10}$	4.6
	Periclase (MgO)	$2.1x10^{12}$	6.3
Mo(III)	H_2MoO_4	$8.0x10^{19}$	13.9
	MoO_3	$5.2x10^{51}$	45.7
Pb(II)	$Pb_3(PO_4)_2$	$3.5x10^{-4}$	-9.5
	Hydroxylpyromorphite ($Pb_5(PO_4)_3(OH)$)	$3.8x10^{-4}$	-9.4
	$PbHPO_4$	$6.6x10^{-4}$	-9.2

	$Pb(OH)_2$	$4.5x10^{-1}$	-6.3
	Hydrocerrusite ($Pb_3(CO_3)_2(OH)_2$)	1.4	-5.9
	Cerrusite ($PbCO_3$)	5.5	-5.3
	Pb_2OCO_3	$2.0x10^{2}$	-3.7
	$Pb_3O_2CO_3$	$4.6x10^{2}$	-3.3
	$Pb_{10}(OH)_6O(CO_3)_6$	$2.2x10^{4}$	-1.7
	Litharge (α -PbO)	$7.0x10^{8}$	2.8
	Massicot (β -PbO)	$4.1x10^{9}$	3.6
	$PbO:O.3H_2O$	$5.8x10^{11}$	5.8
	$Pb_2O(OH)_2$	$1.7x10^{12}$	6.2

Table S9. Saturation index of various precipitates for each metal in SRM1648a samples 1, 2 and 3 under assay conditions (0.1M PO_4, ionic strength=0.22, 37C).

Metal	Solid	Sample 1	Sample 2	Sample 3
Cu(I)	Cuprite (Cu_2O)	2.8	3.7	4.6
Cu(II)	$Cu_3(PO_4)_2$	-5.0	-3.5	-2.2
	Tenorite (CuO)	-2.0	-1.5	-1.1
	$Cu_3(PO_4)_2{:}3H_2O$	-6.7	-5.3	-4.0
	$Cu(OH)_2$	-3.1	-2.6	-2.2
Fe(II)	$Fe_3(PO_4)_2$	-4.4	-2.9	-1.8
	Vivianite ($Fe_3(PO_4)_2{:}8H_2O$)	-4.4	-2.9	-1.8
	Wusite (FeO)	-4.8	-4.4	-4.0
	$Fe(OH)_2$	-7.9	-7.4	-7.0
Fe(III)	Hematite (Fe_2O_3)	14.0	15.0	16.0
	Goethite (ὰ- FeO(OH))	5.8	6.3	6.7
	Lepidocrocite (γ - FeO(OH))	4.5	5.0	5.5
	Strengite ($FePO_4.2H_2O$)	3.6	4.1	4.6
	Ferrihydrite ($Fe_2O_3.0.5H_2O$)	3.2	3.7	4.1
	Maghemite (γ - Fe_2O_3)	5.4	6.4	7.3

Mn(II)	$MnHPO_4$	2.6	3.2	3.7
	$Mn_3(PO_4)_2$	-16.0	-14.2	-12.7
	Pyrochroite ($Mn(OH)_2$)	-8.6	-8.0	-7.6
	Hausmannite ($(Mn^{2+}\ Mn^{3+})_2\ O_4$)	9.9	10.2	10.5
Mn(III)	Manganite ($MnO(OH)$)	3.0	4.6	5.8
	Bixbyite ($(Mn, Fe)_2O_3$)	2.3	2.8	3.2
Mn(IV)	Pyrolusite (MnO_2)	7.6	8.5	9.3
	Nsutite ($Mn^{4+}\ Mn^{2+}O(OH)_2$)	7.3	7.7	7.9
	Birnessite ($(Mn^{4+}\ Mn^{3+})_2O_2.5H_2O$)	6.7	7.1	7.3
Ni(II)	$Ni_3(PO_4)_2$	-8.7	-7.2	-5.7
	Bunsenite (NiO)	-6.0	-5.4	-5.0
	$Ni(OH)_2$	-6.3	-5.8	-5.3
Zn(II)	$Zn_3(PO_4)_2$	-1.5	0.1	1.5
	$Zn(OH)_2$	-5.4	-4.8	-4.4
Cr(III)	Cr_2O_3	3.1	3.7	4.5
	$Cr(OH)_3$ [Am]	1.0	1.3	1.7
	$Cr(OH)_3$	-0.9	-0.6	-0.2
Cr(VI)	CrO_3	-19.1	-18.8	-16.4

Co(II)	$Co_3(PO_4)_2$	-5.5	-4.0	-3.1
	$CoHPO_4$	-3.9	-3.4	-3.1
	CoO	-7.1	-6.6	-6.3
	$Co(OH)_2$	-7.4	-6.8	-6.5
Co(III)	$Co(OH)_3$	11.0	11.5	11.8
V(III)	V_2O_3	-8.7	-8.3	-7.8
	$V(OH)_3$	-11.9	-11.5	-11.0
Al(III)	Diaspore (AlO(OH))	2.2	2.7	3.1
	Gibbsite (γ- $Al(OH)_3$)	0.7	1.2	1.6
	Boehmite (AlO(OH))	0.6	1.0	1.5
	Al_2O_3	-1.2	-0.2	0.7
	$Al(OH)_3$ [Am]	-1.7	-1.2	-0.8
Ca(II)	Hydroxylpatite ($Ca_{10}(PO_4)_6(OH)_2$)	0.9	3.3	5.6
	$Ca_3(PO_4)_2$	-3.3	-1.8	-0.4
	$CaHPO_4$	-1.1	-0.6	-0.2
	$Ca_4H(PO_4)_3{:}3H_2O$	-4.9	-3.0	-1.1
	$CaHPO_4{:}2H_2O$	-1.3	-0.9	-0.4
	Calcite (metastable $Ca(CO_3)$)	-4.6	-4.1	-3.6

	Aragonite ($CaCO_3$)	-4.7	-4.2	-3.8
	Portlandite (metastable $Ca(OH)_2$)	-13.4	-12.9	-12.5
	Lime ($Ca(OH)_2$)	-22.9	-22.4	-21.9
Mg(II)	$MgHPO_4{:}3H_2O$	-2.6	-2.1	-1.6
	$Mg_3(PO_4)_2$	-10.3	-8.8	-7.4
	Magnesite ($MgCO_3$)	-6.4	-5.9	-5.4
	Hydromagnesite ($Mg_5(CO_3)_4(OH)_2.4H_2$)	-36.5	-34.1	-31.8
	Nesquehonite ($MgHCO_3(OH).2H_2O$)	-8.9	-8.4	-7.9
	Artinite ($Mg_2(OH)_2.3H_2O$)	-14.5	-13.5	-12.6
	Brucite ($Mg(OH)_2$)	-8.1	-7.6	-7.2
	$Mg(OH)_2$	-10.8	-10.3	-9.9
	Periclase (MgO)	-12.6	-12.1	-11.7
Pb(II)	$Pb_3(PO_4)_2$	9.2	10.8	12.2
	Hydroxylpyromorphite ($Pb_5(PO_4)_3(OH)$)	15.1	17.9	20.1
	$PbHPO_4$	2.8	3.3	3.8
	$Pb(OH)_2$	-0.1	0.5	0.9
	Hydrocerrusite ($Pb_3(CO_3)_2(OH)_2$)	-1.4	0.2	1.6
	Cerrusite ($PbCO_3$)	-1.0	-0.4	0.0

	Pb_2OCO_3	-5.4	-4.3	-3.4
	$Pb_3O_2CO_3$	-8.8	-7.2	-5.8
	$Pb_{10}(OH)_6O(CO_3)_6$	-44.1	-38.7	-34.2
	Litharge (α -PbO)	-4.6	-4.0	-3.6
	Massicot (β -PbO)	-4.7	-4.2	-3.7
	$PbO{:}O.3H_2O$	-5.3	-4.7	-4.3
	$Pb_2O(OH)_2$	-10.8	-9.7	-8.8